iScience

CellPress
OPEN ACCESS

Article

Neurogenic-dependent changes in hippocampal circuitry underlie the procognitive effect of exercise in aging mice

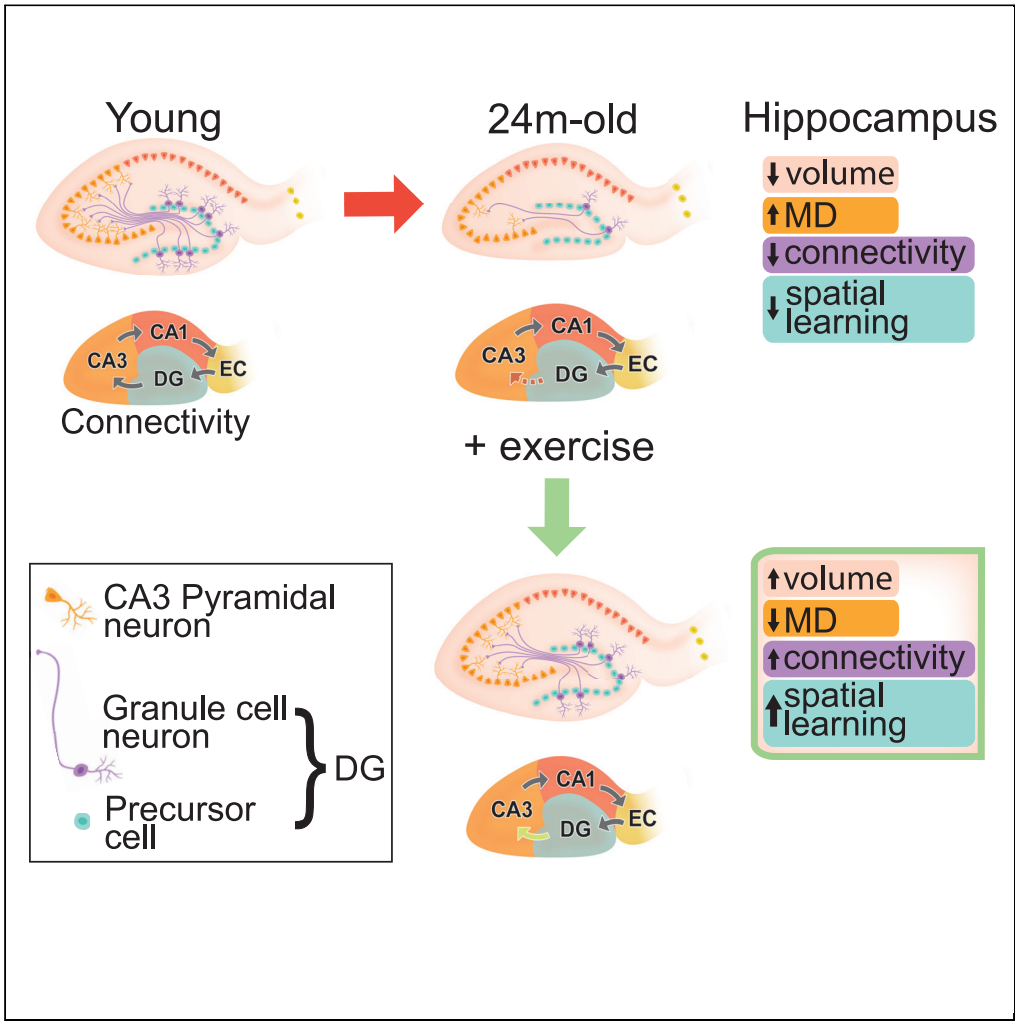

Xiaoqing Alice Zhou, Daniel G. Blackmore, Junjie Zhuo, ..., Kai-Hsiang Chuang, Tianzi Jiang, Perry F. Bartlett

p.bartlett@uq.edu.au (P.F.B.)
jiangtz@nlpr.ia.ac.cn (T.J.)
k.chuang@uq.edu.au (K.-H.C.)

Highlights

Exercise can enhance connectivity in the dorsal hippocampus to improve spatial learning

Circuitry changes depend on increased neurogenesis in the hippocampus of aged animals

Identification of the specific changes in circuitry underlying cognitive improvements

Enhanced connectivity occurs only after exercise of a specific duration: the sweet spot

Zhou et al., iScience 24, 103450
December 17, 2021
https://doi.org/10.1016/j.isci.2021.103450

iScience

CellPress
OPEN ACCESS

Article

Neurogenic-dependent changes in hippocampal circuitry underlie the procognitive effect of exercise in aging mice

Xiaoqing Alice Zhou,[1,4] Daniel G. Blackmore,[1,4] Junjie Zhuo,[1,3] Fatima A. Nasrallah,[1,2] XuanVinh To,[1] Nyoman D. Kurniawan,[2] Alison Carlisle,[1] King-Year Vien,[1] Kai-Hsiang Chuang,[1,2,*] Tianzi Jiang,[1,3,*] and Perry F. Bartlett[1,5,*]

SUMMARY

We have shown that the improvement in hippocampal-based learning in aged mice following physical exercise observed is dependent on neurogenesis in the dentate gyrus (DG) and is regulated by changes in growth hormone levels. The changes in neurocircuitry, however, which may underlie this improvement, remain unclear. Using *in vivo* multimodal magnetic resonance imaging to track changes in aged mice exposed to exercise, we show the improved spatial learning is due to enhanced DG connectivity, particularly the strengthening of the DG-Cornu Ammonis 3 and the DG-medial entorhinal cortex connections in the dorsal hippocampus. Moreover, we provide evidence that these changes in circuitry are dependent on neurogenesis since they were abrogated by ablation of newborn neurons following exercise. These findings identify the specific changes in hippocampal circuitry that underlie the cognitive improvements resulting from physical activity and show that they are dependent on the activation of neurogenesis in aged animals.

INTRODUCTION

The incidence of cognitive decline increases with age, especially for impairments in episodic memory (Nyberg and Pudas, 2019) and spatial memory (Coughlan et al., 2018; Lester et al., 2017), which are typically associated with the hippocampus (Fan et al., 2017). Deterioration in the morphometry of the hippocampus, as well as the integrity of its circuitry, are thought to be critical in the progression of these deficits (Marstaller et al., 2015). There is increasing evidence that some forms of physical exercise protect against spatial memory decline; however, the results have been inconsistent in both humans (Cooper et al., 2013; Livingston et al., 2017; Sofi et al., 2011) and animals (Creer et al., 2010; Marlatt et al., 2012; van Praag et al., 2005). Although several explanations have been proposed (Livingston et al., 2017; Moon et al., 2016; Sleiman et al., 2016; van Praag, 2008), the precise mechanism(s) by which exercise improves brain health remain unclear. We recently demonstrated that an optimal period of exercise in aged mice is required to activate neurogenesis in a growth hormone-dependent manner, resulting in the restoration of hippocampal-dependent spatial learning (Blackmore et al., 2021). What remains elusive, however, is how the structure and functional circuitry of the hippocampus is remodeled and what drives these connectivity changes following exercise in the aged brain.

In studies showing that adult hippocampal neurogenesis (AHN) leads to cognitive changes during aging, little has been reported about how exercise affects the structure and functional circuitry responsible for behavioral changes, and whether any circuitry changes are dependent on the level of neurogenesis. Magnetic resonance imaging (MRI) studies in humans have revealed that older adults show significant increases in hippocampal volume (Erickson et al., 2011) and functional connectivity (Reagh et al., 2018) after aerobic exercise intervention. Similarly, rodent MRI studies have demonstrated that running increases hippocampal volume (Biedermann et al., 2012) and blood flow (Pereira et al., 2007). However, the specific circuitry related to improved cognition and whether this is directly regulated by neurogenesis remain unknown.

To address these issues, we applied structural, diffusion, and functional MRI (fMRI) longitudinally following different periods of exercise in mouse models. We hypothesized that behavioral performance in aged mice

[1]Queensland Brain Institute, The University of Queensland, Brisbane, QLD 4072, Australia

[2]Centre for Advanced Imaging, The University of Queensland, Brisbane, QLD 4072, Australia

[3]Brainnetome Center, Institute of Automation, Chinese Academy of Sciences, Beijing 100190, China

[4]These authors contributed equally

[5]Lead contact

*Correspondence: p.bartlett@uq.edu.au (P.F.B.), jiangtz@nlpr.ia.ac.cn (T.J.), k.chuang@uq.edu.au (K.-H.C.)

https://doi.org/10.1016/j.isci.2021.103450

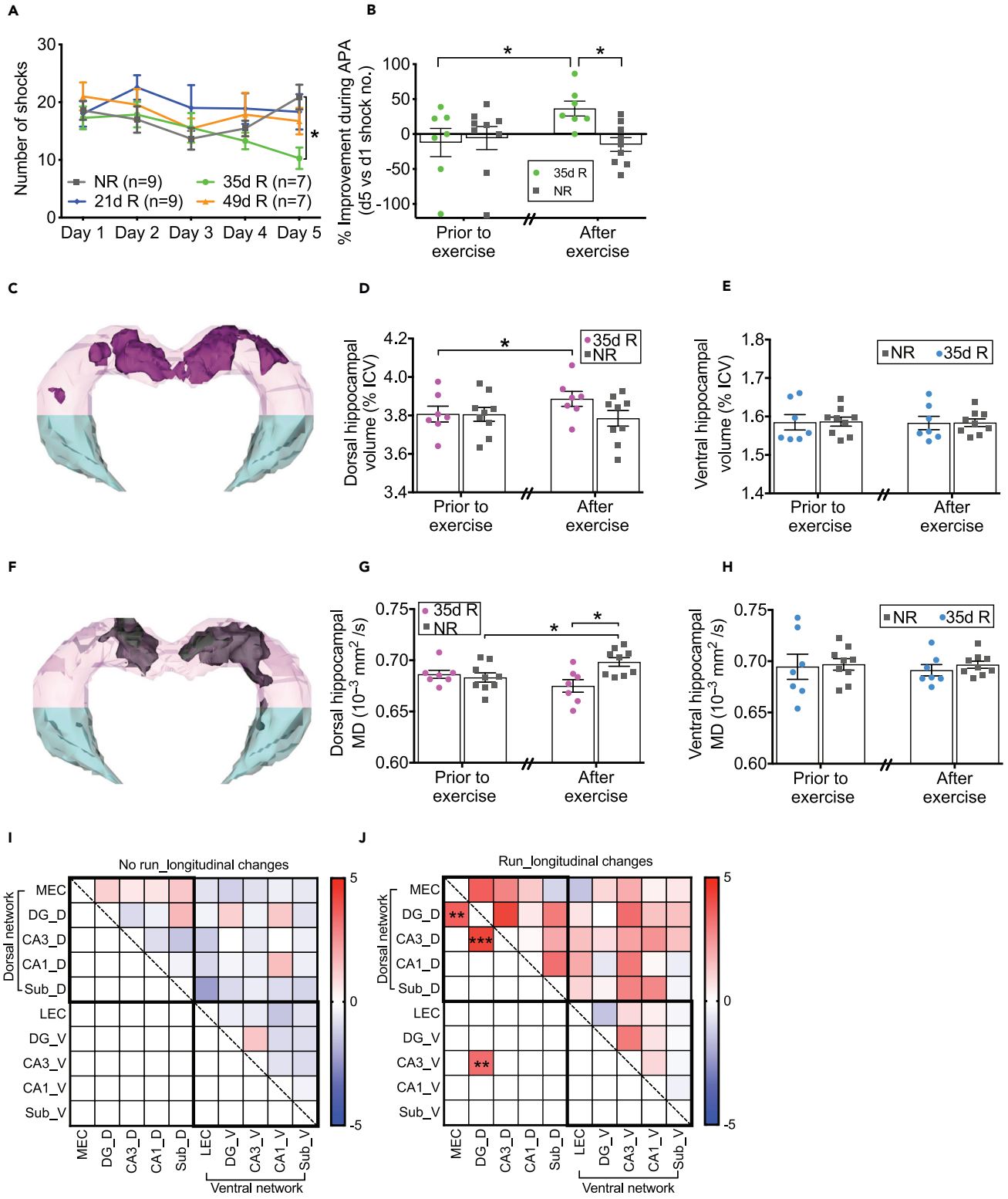

Figure 1. Optimal voluntary physical exercise restores hippocampal structure and function in 24-month-old animals

(A) 35 days of exercise resulted in a significant decrease in shock number during the APA test, with shorter or longer periods having no effect (mean ± SE, two-way RM-ANOVA with false discovery rate [FDR] posthoc tests).

Figure 1. *Continued*

(B) 35 days of exercise resulted in spatial learning improvement, as calculated by the difference from day 1–5, represented as a percentage (mean ± SE; two-way repeated measures ANOVA with FDR posthoc tests).

(C) 3D rendering of the hippocampus, with the dorsal hippocampus represented in light pink and the ventral hippocampus represented in light blue. The spatial distributions of the exercise-mediated volumetric changes (represented in dark pink) were overlaid, revealing that increased volume was restricted to the dorsal hippocampus.

(D) The dorsal hippocampal volume was significantly increased after exercise (mean ± SE; two-way RM-ANOVA treatment and time interaction [$F(1,14) = 9.054$, $^{*}p < 0.05$], with FDR posthoc tests).

(E) The ventral hippocampal volume showed no significant changes after exercise.

(F) The spatial distribution of age-related MD changes (represented in gray) were overlaid and revealed that the increase in MD value in the no run group was restricted to the dorsal hippocampus.

(G) The dorsal hippocampal MD value increased in the no run group mean ± SE; two-way RM-ANOVA treatment and time interaction [$F(1,14) = 11.996$, $^{*}p < 0.05$], with FDR posthoc tests).

(H) The ventral hippocampal MD value showed no significant changes for either group.

(I) The correlation matrices among hippocampal regions in the no run group compared with their individual baseline (paired-sample t test, uncorrected). The upper triangle shows the raw t-score, and the lower triangle reveals the significant increase in sub-region-specific connections that survived statistics. No connection matrices were significant in the no run group. The color scale indicates the z values.

(J) The correlation matrices among hippocampal regions in the 35-day run group compared with their individual baseline (paired-sample t test, uncorrected). The dorsal DG-CA3 and dorsal DG-MEC connections were significantly enhanced in the runner group. NR, no run; R, run; ICV, intracranial volume; MD, mean diffusivity. $^{**}p < 0.01$,$^{***}p < 0.001$.

See also Figure S1.

depends on dentate gyrus (DG) connectivity driven by exercise-induced neurogenesis. To determine the contribution of AHN to this process, we specifically ablated doublecortin (DCX)-positive newborn neurons using our novel knockin DCX^{DTR} mouse line (Vukovic et al., 2013). Our results reveal that improved spatial learning in aged mice after exercise is due to enhanced DG connectivity, particularly the strengthening of the DG-Cornu Ammonis 3 (CA3) and the DG-medial entorhinal cortex (MEC) connections in the dorsal hippocampus. Moreover, we provide evidence that this change in circuitry is dependent on the activation of neurogenesis.

RESULTS

Spatial learning performance is dependent on exercise duration

We first confirmed our previous data that only the mice that had run for 35 days showed significant improvement in active place avoidance (APA) performance, as indicated by a decrease in shock number, whereas shorter or longer periods of exercise had an insignificant effect on learning ability (Figure 1A). The learning performance was then calculated as a percentage based on the number of shocks received on the last day compared with the first day of APA testing. Only those animals that underwent 35 days of physical exercise displayed an improvement in spatial learning ability relative to no run controls (Figures 1B and S1A–S1C). Although we focused primarily on shock number, other components including time to first entrance and maximum time spent avoiding the shock zone were also compared during the testing period. We found that only the animals that underwent the optimal 35-day period of exercise exhibited an increase in time to first entrance and the maximal time avoiding the shock zone as the test continued, demonstrating that spatial learning improved following exercise. The no run controls and those animals that underwent either 21- or 49-day exercise periods, however, showed no improvement during testing (Figures S1D and S1E). We also showed that cognition improved to a level that resembled the performance of younger animals that had not been exposed to exercise (Figure S1F).

Physical exercise alters hippocampal structure and function in the aged murine brain

It has been demonstrated that the hippocampus is involved in learning and memory (Buzsaki and Moser, 2013; Fan et al., 2017), and studies have reported that the dorsal hippocampus is critical for successful spatial learning (Moser et al., 1993, 1995). We initially investigated structural and functional changes in the whole hippocampus, after which we compared the relative contributions of the dorsal and ventral hippocampal sub-regions longitudinally following exercise in 24-month-old mice. The experimental design used to assess the longitudinal hippocampal changes before and after exercise is shown in Figure S1G.

High-resolution structural MRI was used to subdivide the hippocampus into dorsal and ventral regions *in vivo* (Figure S1H). A morphometry analysis was applied to determine the volumetric change after exercise. A 3D rendering of the hippocampus was produced, with the spatial distribution of the exercise-mediated volumetric changes overlaid. This revealed that only the dorsal hippocampus increased in volume

(Figures 1C–1E). Regional analysis confirmed that exercise significantly increased the volume of the dorsal hippocampus, with posthoc analysis revealing that exercise significantly increased the dorsal hippocampal volume relative to the baseline value before exercise (Figure 1D). The volume of the ventral hippocampus was not affected (Figure 1E).

The microstructure of the hippocampus was assessed by measuring the mean diffusivity (MD) using diffusion tensor imaging (DTI). It has been suggested that MD is a sensitive surrogate of cell density in tissue, with an increase in MD indicative of reduced cell density (Le Bihan, 2014). We observed an age-dependent MD increase specifically in the dorsal hippocampus of no run animals (Figures 1F–1H). Detailed analysis confirmed that the MD values increased in the dorsal hippocampus (Figure 1G), but not the ventral hippocampus (Figure 1H), in aged mice. This result indicates that exercise protects the integrity of the dorsal hippocampal microstructure.

In concert with the structural changes, we also found that physical exercise altered the hippocampal functional connectivity in the aged brain as measured by resting-state fMRI. The no run group displayed no change over the intervention period, whereas the exercise group demonstrated increased connectivity within the hippocampal circuits, specifically between the MEC and dorsal DG, between the dorsal DG and the dorsal CA3 region, and between the dorsal DG and the ventral CA3 region, all of which have been demonstrated to be involved in spatial learning ability and the consolidation of spatial information (Figures 1I and 1J).

Hippocampal structural and functional changes correlate with behavior and neurogenesis

We next examined the relationship between hippocampal volume, connectivity, and spatial learning performance using Pearson correlations between these readouts at the level of the runner group. Investigation of the hippocampal microstructure change in the dorsal hippocampus revealed a trend toward correlation with spatial learning ability in the runners (Figure 2A). We also found a significant positive correlation between the dorsal DG-CA3 functional connectivity change and spatial learning performance for the runner group (Figure 2B). Thus, decreased MD and greater connectivity in the dorsal DG-CA3 circuit are the key components associated with improved spatial learning performance.

We then used the immature neuron marker DCX to quantify the number and location of adult-born neurons (Figures 2C and 2D), revealing that exercise significantly increased the DCX^{+ve} cell number in the dorsal hippocampus but not the ventral hippocampus (Figure 2C). $DAPI^{+ve}$ cell counts showed that exercise increased the total cell number in the dorsal granule cell layer (GCL) compared with the control group (Figure 2E). Importantly, using our longitudinal high-resolution MRI of brain structure and connectivity, it was also possible to compare these MRI readouts with traditional immunohistochemical data (Figure S2). This analysis revealed that $DAPI^{+ve}$ cell number significantly correlated with MRI MD value (Figure 2F), with the increase in DCX^{+ve} cell number being significantly associated with improved spatial learning ability (Figure 2G) and decreased dorsal hippocampal MD (Figure 2H). There was also a strong correlated trend between increased functional connectivity in the dorsal DG-CA3 circuit and DCX^{+ve} cell number (Figure 2I).

To address whether non-optimized periods of exercise have the same beneficial effect on hippocampal structure and connectivity, we examined 24-month-old animals that exercised on a running wheel for periods of 21 or 49 days. Examination of the hippocampus from these animals revealed no discernible effect in terms of hippocampal volume, MD, functional connectivity, or DCX^{+ve} cell number (Figure S3).

Together, these results indicate that the improved behavior resulting from physical exercise depends on change in hippocampal structure, functional connectivity, and neurogenesis in the aged murine brain.

Ablation of neurogenesis in young adult mice results in the hippocampal structural and functional changes typically observed in aged brains

To examine the effect of neurogenesis on hippocampal structure and function, we first assessed these changes in 15-week-old (young adult) and aged animals, as aged animals generate minimal new neurons (Bizon and Gallagher, 2003; Sorrells et al., 2018). We compared 15-week-old mice with 24 month-old mice and found that the aged group displayed a significant decrease in hippocampal neurogenesis in both the dorsal and ventral hippocampal regions (Figure 3A). The aged group also displayed a significant decrease in dorsal hippocampal volume (Figure 3B) and an increase in dorsal hippocampal MD (Figure 3C) compared with the 15-week-old group. In agreement with the structural impairment, aging also resulted in weaker

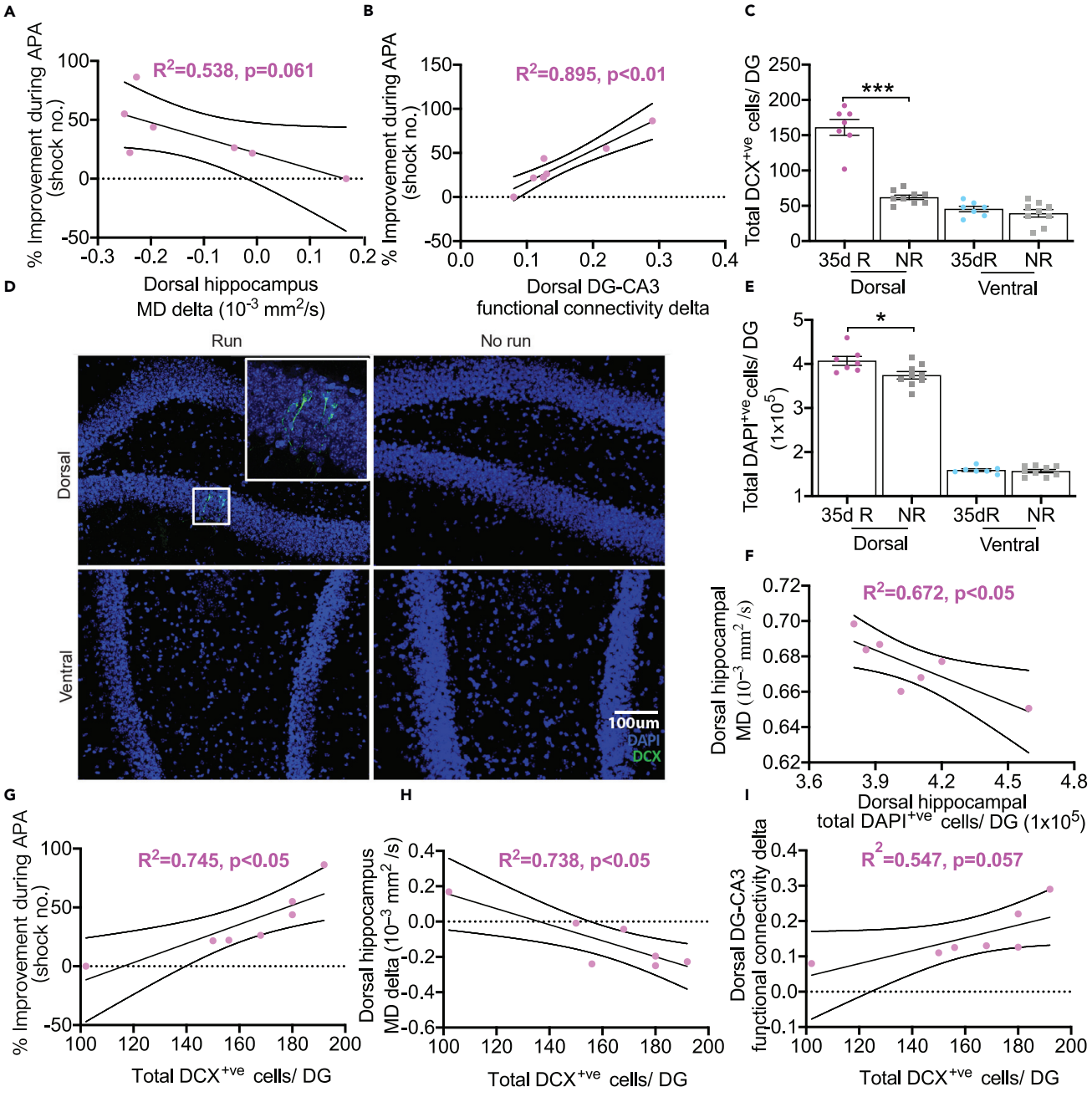

Figure 2. Increased neurogenesis in the dorsal hippocampus is associated with structural and functional changes and improved spatial learning ability

(A and B) (A) Spatial learning ability (the difference from day 1–5, represented as a percentage) negatively correlated with MD value (R^2 = 0.538, p = 0.061) and (B) positively correlated with DG-CA3 connectivity (R^2 = 0.895, p < 0.01).

(C) Exercise increased the number of immature neurons (DCX^{+ve} cells) in the dorsal DG (mean ± SE, independent two-sample t test [t(14) = 9.441], ***p < 0.001).

(D) Representative images for DCX^{+ve} cells.

(E) Exercise increased the total cell number ($DAPI^{+ve}$ cells) in the dorsal GCL of the DG (mean ± SE, independent two-sample t test, t(14) = 2.509, *p < 0.05).

(F) The $DAPI^{+ve}$ cell number negatively correlated with MD (R^2 = 0.672, p < 0.05).

(G) The DCX^{+ve} cell number positively correlated with spatial learning ability (R^2 = 0.745, p < 0.05).

(H and I) (H) The DCX^{+ve} cell number negatively correlated with MD delta (R^2 = 0.738, p < 0.05) and (I) positively correlated with DG-CA3 connectivity delta (R^2 = 0.547, p = 0.057). The correlations were calculated in the runner group.

See also Figures S2 and S3.

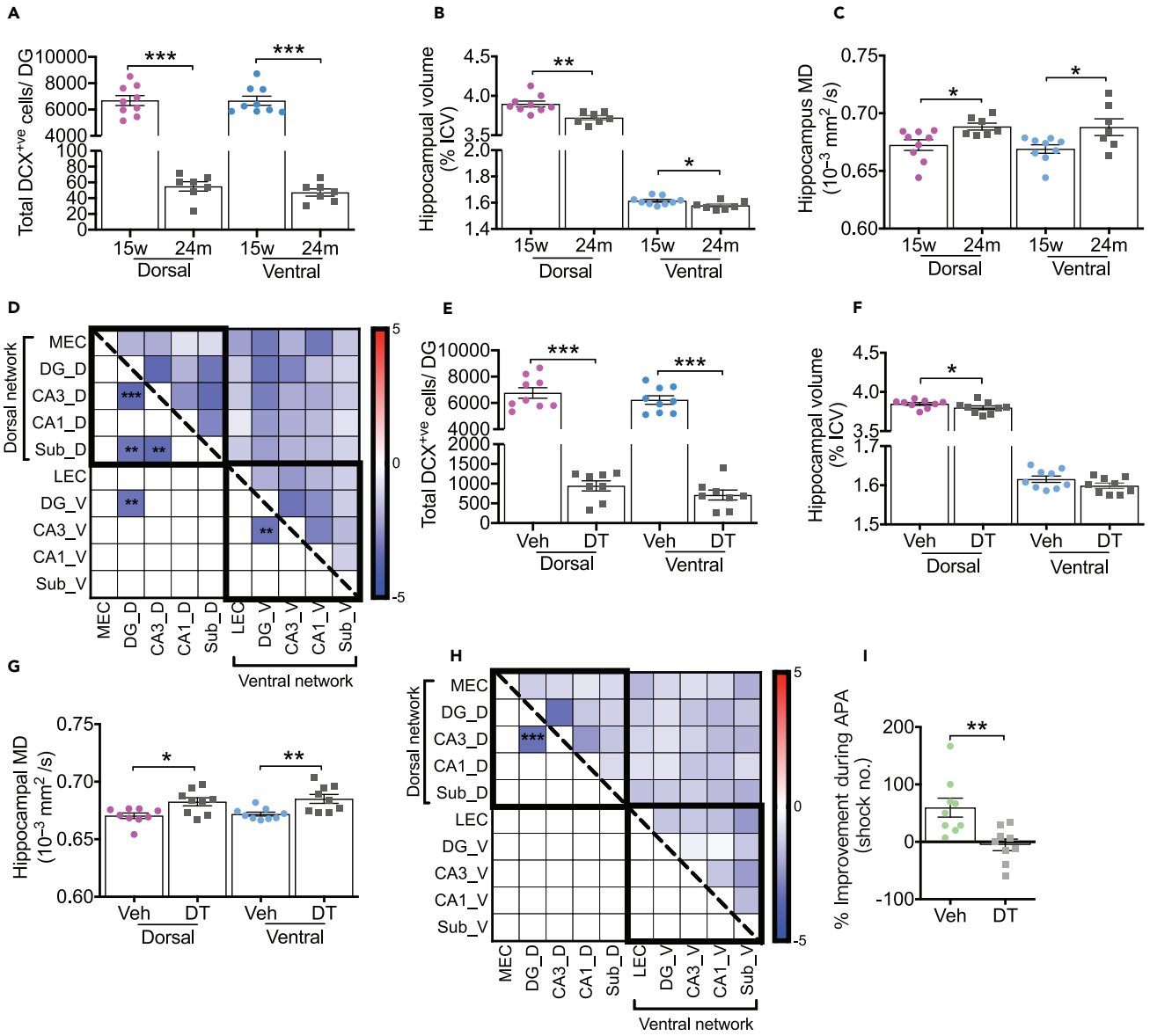

Figure 3. Neurogenesis depletion changes hippocampal structure and functional connectivity in young animals

(A) The 24-month group showed significant differences in the number of DCX^{+ve} cells in both the dorsal and ventral hippocampal regions relative to young animals (mean ± SE, independent two-tailed t test; $t(14) = 12.26$, $p < 0.001$ and $t(14) = 5.54$, $p < 0.001$, respectively).

(B) The volume of both the dorsal and ventral hippocampal regions significantly decreased in naive old animals compared with the naive young group (mean ± SE, independent two-tailed t test; $t(14) = 3.638$, $p < 0.01$).

(C) The MD in both the dorsal and the ventral hippocampal regions increased in naive old animals when compared with the naive young group (mean ± SE, independent two-tailed t test; $t(14) = 2.685$, $p < 0.05$).

(D) The functional connectivity of the dorsal DG-CA3, dorsal DG-subiculum, dorsal DG-ventral DG, dorsal CA3-subiculum, and ventral DG-CA3 connections were significantly decreased in the old mice compared with young mice (independent two-tailed t test, uncorrected).

(E) DT treatment decreased the number of DCX^{+ve} cells in both the dorsal and ventral hippocampal regions in young DCX^{DTR} mice (mean ± SE, independent two-tailed t test $t(15) = 15.33$, $p < 0.001$ and $t(15) = 16.8$, $p < 0.001$, respectively).

(F) The volume of the dorsal hippocampus decreased significantly in the DT-treated DCX^{DTR} group compared with the vehicle-treated group (mean ± SE, independent two-tailed t test; $t(16) = 2.596$, $p < 0.05$).

(G) The MD of both the dorsal and ventral hippocampal regions increased significantly in the DT-treated DCX^{DTR} group compared with the vehicle-treated group (mean ± SE, independent two-tailed t test; $t(16) = 2.892$, $p < 0.05$ and $t(16) = 3.150$, $p < 0.01$, respectively).

(H) The functional connectivity of the dorsal DG-CA3 connection significantly decreased in the DT-treated DCX^{DTR} mice compared with vehicle-treated DCX^{DTR} mice (independent two-tailed t test, uncorrected).

Figure 3. *Continued*
(I) The vehicle-treated DCX^{DTR} group showed improvement in spatial learning (the difference from day 1–5, represented as a percentage), whereas DCX^{DTR} mice injected with DT showed no improvement in spatial learning (mean ± SE, independent two-tailed t test). *p < 0.05, **p < 0.01, ***p < 0.001.
See also Figure S4.

connectivity within the hippocampus compared with that in 15-week-old animals, specifically between the dorsal DG and dorsal CA3, between the dorsal DG and dorsal subiculum, between the dorsal DG and ventral DG, between the dorsal CA3 and dorsal subiculum, and between the ventral DG and ventral CA3 (Figure 3D), which were the same regions in which an improvement was observed in aged animals following an optimal period of exercise.

We next examined the link between hippocampal neurogenesis and hippocampal structure and function in young mice. To specifically ablate adult-born neurons we used naive 15-week-old transgenic DCX^{DTR} mice in which immature neurons (DCX^{+ve}) express the human diphtheria toxin (DT) receptor (DTR). Upon administration of DT new neurons can be selectively ablated (Vukovic et al., 2013). We randomly divided the animals into either a DT or a control vehicle injection group. Following treatment, these mice were scanned to evaluate their hippocampal structure and function. A significant decrease in neurogenesis was found in both the dorsal and ventral hippocampus (Figure 3E). The neurogenesis ablation group displayed a volume decrease in the dorsal hippocampus (Figure 3F), but not the ventral hippocampus, as well as an increase in MD values in both the dorsal and ventral hippocampal regions (Figure 3G) when compared with the control group. In agreement with the observed structural impairment, the ablation group also displayed decreased functional connectivity between the dorsal DG and dorsal CA3 (Figure 3H). Cognitively, the neurogenesis ablation group showed no improvement in spatial learning, and performed significantly worse than intact animals in the APA task (Figure 3I).

To exclude any confounding effect of DT injection, we also examined its impact on the hippocampal features and learning ability of a group of wild-type mice. This analysis revealed no significant change in cognitive performance or hippocampal features in response to DT injection, and no decrease in the number of newborn neurons (Figure S4).

Importantly, both the naturally aged mice and the 15-week-old animals in which neurogenesis was ablated displayed a dorsal hippocampal volume decrease and an MD increase. The dorsal DG-CA3 functional connectivity also decreased in both groups. These results suggest that the decrease in hippocampal neurogenesis is a key factor in the structural and functional deterioration of the hippocampus.

Neurogenesis underlies the structural and functional changes in the hippocampus

Having established that age-related hippocampal structure and function can be restored by optimal physical exercise, and that adult neurogenesis is linked to this outcome, we next investigated whether these processes are directly linked. To achieve this, we used aged DCX^{DTR} mice in which the deficit in new neurons can be restored in response to physical exercise (Blackmore et al., 2021). As before, to stimulate neurogenesis, all mice had access to a running wheel for a period of 35 days. We then divided the animals randomly into either a DT or vehicle injection group. After injection, the mice were scanned to evaluate hippocampal structure and function. The ablation group displayed a significant decrease in neurogenesis in the dorsal hippocampus (Figures 4A and 4B). Structurally, this group also exhibited a significant dorsal hippocampal volume decrease (Figures 4C and 4D), as well as a significant dorsal hippocampal MD increase (Figures 4E and 4F), when compared with the control group. In agreement with the structural impairment, the ablation group also displayed decreased functional connectivity between the dorsal DG and dorsal CA3 regions (Figure 4G; $p < 0.001$, uncorrected). In addition, this group showed no improvement in spatial learning, as evidenced by receiving the same number of shocks for each day of APA testing, as opposed to the control group that received fewer shocks as the test progressed (Figure 4H). Importantly, the hippocampal structure and function pattern of the ablation group resembled that of naive aged animals that had not exercised. These results identify an increase in hippocampal neurogenesis as a key factor in the structural and functional changes that occur in response to exercise.

DISCUSSION

Using longitudinal, multimodal MRI, we demonstrate that exercise-mediated improvements in spatial learning in 24-month-old female mice are due to changes in hippocampal structure and function. This

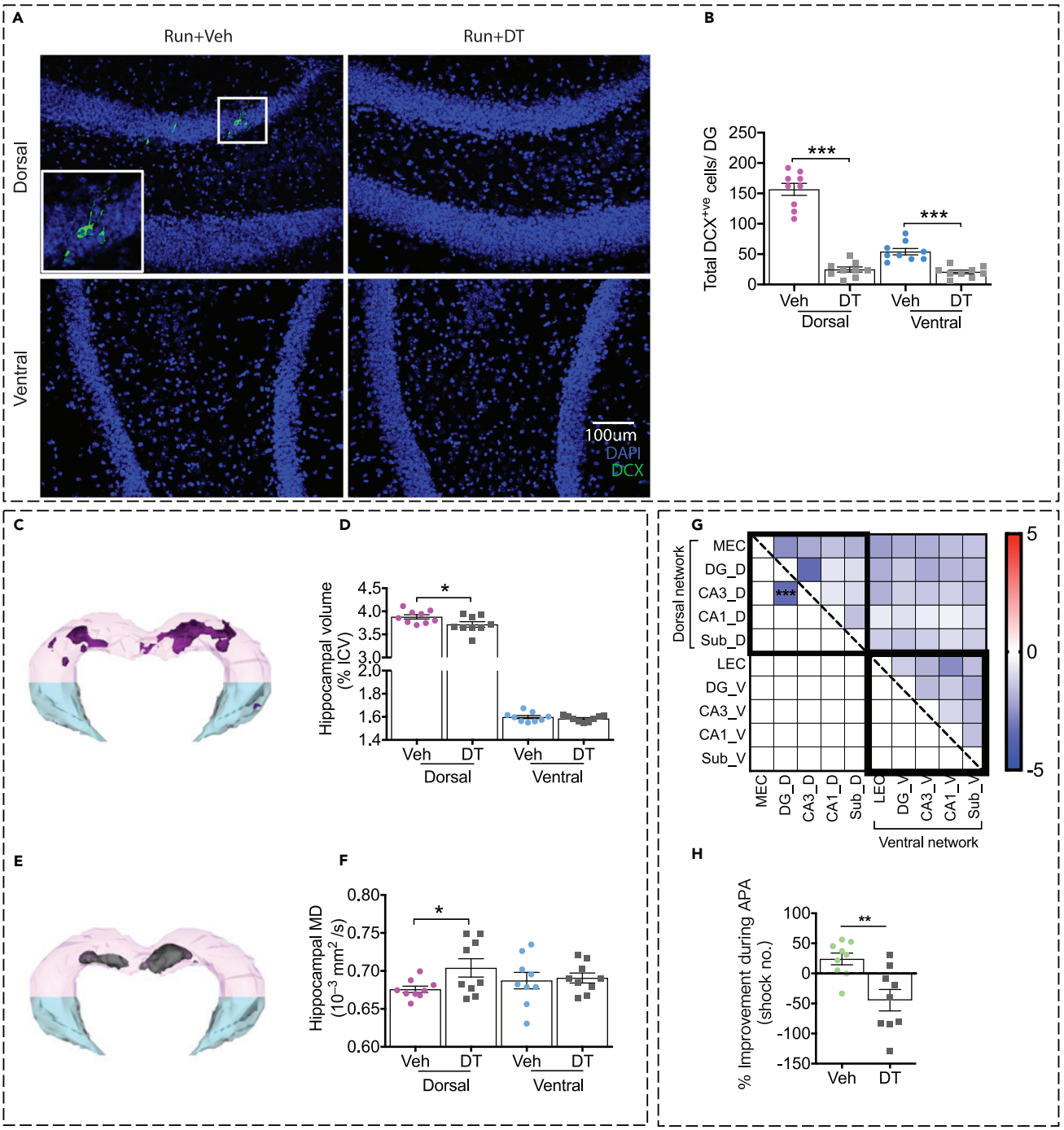

Figure 4. Neurogenesis depletion abolishes exercise-mediated hippocampal structural and functional benefits in 24-month-old animals

(A) Representative image for DCX^{+ve} cells in 24-month 35-day run DCX^{DTR} mice.

(B) DT treatment decreased the number of DCX^{+ve} cells in the dorsal hippocampus in 24-month 35-day run DCX^{DTR} mice (mean ± SE, independent two-tailed t test; $t(16) = 12.26$, $p < 0.001$).

(C) 3D rendering of the hippocampus, with the dorsal hippocampus represented in light pink and the ventral hippocampus represented in light blue. The spatial distributions of the volumetric changes (represented in dark pink) were overlaid and revealed that only the dorsal hippocampus increased in volume.

(D) The volume of the dorsal hippocampus decreased significantly in the DT-treated DCX^{DTR} group when compared with the vehicle-treated group (mean ± SE, independent two-tailed t test; $t(16) = 2.144$, $p < 0.05$).

(E) The spatial distributions of the MD changes (represented in gray) were overlaid and revealed that only the dorsal hippocampus exhibited an increased MD value.

Figure 4. *Continued*

(F) The MD of the dorsal hippocampus increased significantly in the DT-treated DCX^{DTR} group when compared with the vehicle-treated group (mean ± SE, independent two-tailed t test; $t(16) = 1.811$, $p < 0.05$).

(G) The dorsal DG-CA3 functional connectivity in the DT-treated mice decreased compared with that in the vehicle-treated mice (independent two-tailed t test, uncorrected).

(H) Following physical exercise, mice injected with vehicle showed an improvement in spatial learning (the difference from day 1–5, represented as a percentage), whereas mice injected with DT displayed no improvement (mean ± SE, independent two-tailed t test; $t(16) = 3.395$, $p < 0.01$). *$p < 0.05$, **$p < 0.01$, ***$p < 0.001$.

includes an increase in hippocampal volume, specifically within the dorsal hippocampus. There was a concomitant increase in immature DCX^{+ve} neurons, also restricted to the dorsal hippocampus. Resting-state fMRI highlighted the exercise-mediated enhancement of key circuitry components including between the dorsal DG and CA3 and the dorsal DG and MEC. Importantly, these changes only occurred following an optimal period of exercise with both shorter and longer exercise being ineffective. By using a separate cohort of 24-month-old mice this study confirms the presence of an optimal exercise period, highlighting the robustness of the model we reported earlier (Blackmore et al., 2021). Critically, the identification of a specific, hippocampal-enhancing period of exercise allowed us to define the mechanisms occurring within the aged brain and shows that reinstating key hippocampal circuitry lost during physiological aging drives spatial learning improvements.

Female mice were chosen for ease of long-term group housing as they are less likely to fight and therefore do not require prolonged separation and single housing, which is well established to cause separation anxiety and stress. Importantly, the positive effects of exercise including increasing hippocampal proliferation, neurogenesis, and spatial learning was originally demonstrated using female mice (van Praag et al., 1999a, 1999b). Furthermore, previous studies have shown no differences between sexes in terms of exercise-mediated hippocampal proliferation (Ma et al., 2012), whereas others combined the data from males and females when examining changes in cognitive function (Sahay et al., 2011). Using 24-month-old female mice, we first wished to determine, both at the macroscopic and microscopic levels, what changes occur within the hippocampus following exercise that mediate the observed cognitive improvements. We found that physical exercise selectively increased the volume of the dorsal hippocampus, a region described as being critical for spatial learning and memory (Kheirbek et al., 2013; Moser et al., 1993, 1995), whereas no change was observed in the ventral hippocampus. Correlation analysis found that spatial cognitive performance was significantly associated with these changes in the dorsal hippocampus. Although it has been reported that running increases AHN specifically in the dorsal hippocampus (Vivar et al., 2016), and an *ex vivo* MRI study indicated volume increase occurs predominantly in the same region (Cahill et al., 2015), the contribution to exercise-mediated changes in the dorsal hippocampus to behavioral improvement remained speculative. Our results therefore suggest that an increase in dorsal hippocampal volume could be an endophenotypic indicator of the efficacy of exercise in enhancing cognitive ability.

Our finding that the dorsal and ventral hippocampal regions are differentially affected adds to a wealth of evidence, including lesion, genetic expression, and tracer studies, as well as fMRI, which have suggested that the hippocampus is functionally segregated along its longitudinal axis into dorsal and ventral regions in rodents, and analogous posterior and anterior regions in monkeys and humans (Fanselow and Dong, 2010; Strange et al., 2014). Moreover, lesion (Moser et al., 1993, 1995), electrophysiology (Jung et al., 1994), optogenetic (Kheirbek et al., 2013), and fMRI (Greicius et al., 2003) studies have indicated that the dorsal hippocampus and related networks are the components that are critical for spatial memory and learning, whereas the ventral region is associated with emotional processing (O'Leary and Cryan, 2014; Squire, 1992). Importantly, the APA test we employed has been shown not to increase cortisol levels (Lesburgueres et al., 2016), indicating that the ventral hippocampus and amygdala are not heavily involved and inactivation of the dorsal hippocampus using tetrodotoxin (Cimadevilla et al., 2000) prevented spatial learning ability during APA testing.

We next moved to identify the causal factors of increased hippocampal volume. We show that there was an increase in immature, DCX^{+ve} neurons following the optimal period of 35-d exercise, as we (Blackmore et al., 2021) and others have reported (van Praag et al., 2005; Wu et al., 2015). Further analysis confirmed that, as with our high-resolution structural MRI data, the increase in DCX^{+ve} neurons was restricted to the dorsal hippocampus. In concert with both an increase in dorsal hippocampal volume and DCX^{+ve} neurons was a change in MD within the same region. Alterations in MD value have been associated with changes in both

tissue density (due to reshaping of neuronal or processes) (Biedermann et al., 2016; Sagi et al., 2012) and enhancement of tissue organization (strengthening of axonal or dendritic backbones and surrounding tissue) (Gomez et al., 2017). The decrease in MD value following optimal exercise indicated an increase in tissue density, a finding confirmed by the histology readings of total cell count and cell density. Importantly, we then confirmed that exercise-mediated neurogenesis correlated with larger DG volume and increased cell density. The GCL and DG volume we report were both measured using histology, and the subgranular zone was included in the GCL measurement. Thus, it is likely that the difference in dorsal DG volume is mainly attributable to an increase in volume within the hilus area. This is likely due to an increase in vascularization that has previously been reported (Creer et al., 2010; Leardini-Tristao et al., 2020) and discussed below. However, since it is difficult to precisely determine the subgranular zone extent, which may extend into the hilus, it is possible that some of the increase is attributable to changes here reflecting the increased proliferation seen in the runners.

Given that the absolute number of adult-born neurons is low, particularly in aged animals, how the subtle increase in DCX^{+ve} neurons contributes to macroscopic hippocampal morphometry and function has remained obscured. To unequivocally demonstrate the integral role of neurogenesis in these hippocampal improvements we specifically ablated the exercise-mediated DCX^{+ve} neurons using our novel DCX^{DTR} mice (Vukovic et al., 2013). Ablation following exercise in this way led to the complete abrogation of exercise-mediated hippocampal volumetric and connectivity changes and the inhibition of spatial learning when compared with exercised mice injected with vehicle (increased neurogenesis), as we had observed previously (Blackmore et al., 2021). Furthermore, ablation of DCX^{+ve} neurons in 15-week-old DCX^{DTR} mice also resulted in reduced spatial learning ability, hippocampal volume, and connectivity, mimicking what occurs in physiologically aged mice. Taken together, our study demonstrates that neurogenesis drives local structural and global functional changes in the hippocampus in both young and aged mice.

It has been proposed that newborn neurons recruited into pre-existing neuronal circuits (Vivar et al., 2016) can produce global network changes (Pereira et al., 2007). We provide direct evidence that neurogenesis is critical for dorsal DG-related functional connectivity as measured by fMRI. Specifically, we found that the optimal period of exercise enhanced the dorsal DG-related network, particularly between the MEC-dorsal DG and the dorsal DG-CA3 regions. The increased connectivity of both these circuits was also significantly associated with spatial learning and memory. In line with a recent human study, we did not find a change in MEC-dorsal DG connectivity during physiological aging (Berron et al., 2018), whereas exercise enhanced this pathway in aged mice. The importance of these circuits, especially the DG-CA3 circuit, is further highlighted when comparing paradigms whereby connectivity is reduced. This includes physiological aging, following non-optimal exercise and ablation of DCX^{+ve} neurons in 15-week-old animals, all of which demonstrated a decrease in connectivity in the dorsal DG-CA3 regions and subsequent deficits in spatial learning. These findings add to previous neuroanatomical tract-tracing studies, which revealed that the DG-CA3 connection is the critical information pathway/circuit within the hippocampus (Brun et al., 2002; Nakazawa et al., 2002; Small et al., 2011). Moreover, optogenetic (Bernier et al., 2017; Denny et al., 2014), electrophysiological (Yassa et al., 2011), and fMRI studies (Reagh et al., 2018; Yassa et al., 2010) have all consistently shown that this circuit is essential for spatial processing.

Previous reports have shown that exercise also leads to a substantial amount of synchronized neuroplasticity including numerous cellular and molecular mechanisms directly related to neurogenesis, as well as possible changes in blood flow and vasculature that contribute to the observed volume changes. For example, one recent study (Leardini-Tristao et al., 2020) found that following exercise, the capillary density in the rat brain increases from less than $300/mm^2$ to over $400/mm^2$, the vessels covered by astrocytes in the CA1 region of the hippocampus increase from 5% up to 15%, the number of microglial processes in the CA1 region increases from 25 cells/field to 35 cells/field, and the total vessel length increases from 2 to 4 mm in the hippocampus. Furthermore, in a study of auditory fear conditioning, a higher spine density could explain 20% of the increased volume in the auditory cortex of mice (Keifer et al., 2015). These local changes would also contribute to the macroscopic volume change promoted by neurogenesis (Asan et al., 2021; Biedermann et al., 2012; Keifer et al., 2015).

Translation of rodent studies to the human condition

It is now generally agreed that there is an age-dependent decrease in hippocampal proliferation and neurogenesis rates across mammalian species including rodents (van Praag et al., 2005), dogs (Pekcec et al., 2008) and non-human primates including both macaque (Jabes et al., 2010) and rhesus monkeys (Ngwenya et al.,

2015). Recently, however, there has been renewed discussion regarding the presence of hippocampal neurogenesis in the aged human brain. Out of necessity, studies in humans have primarily focused on examining postmortem samples using immunohistochemical techniques. Differences in experimental approach, including the time at which the sample was collected postmortem, the disease state of the participant, the fixation process used, and the specific cellular markers examined, have resulted in inconsistent results, with some (Sorrells et al., 2018) concluding that hippocampal neurogenesis is absent in aged brains, whereas others report the opposite (Boldrini et al., 2018). Unfortunately, there are few instances where it has been possible to determine if proliferation occurs postnatally in human subjects. One exception to this was a study in which patients with cancer were injected with bromodeoxyuridine (BrdU) before death, revealing several $BrdU^{+ve}$ cells in the hippocampus that co-labeled for neuron-specific markers (Eriksson et al., 1998). An alternative to immunohistochemical analysis is a modified carbon dating approach conducted on brain tissue by Spalding et al. (2005, 2013), which demonstrated that neural cells were younger than birth date, indicating that cell division had occurred postnatally. The authors did not, however, purify the cells, making it impossible to identify cell type. Thus, the presence of neurogenesis in aged humans remains contested.

Animal models provide the ability to target and manipulate specific neural cells or circuits by taking advantage of techniques that are not possible with human participants. Results garnered from these animal studies can then be used to provide direction and less invasive approaches to examine the human brain. The aged mouse model has revealed that hippocampal precursor proliferation and neurogenesis decrease to negligible levels with age (Kronenberg et al., 2006). Our data (here and Blackmore et al., 2021) for naive 24-month-old mice support such a reduction and are therefore comparable to studies that posit minimal neurogenesis in the aged human hippocampus (Sorrells et al., 2018). Specific ablation of immature neurons in young mice mimics two major components of the aging brain: a lack of neurogenesis and deficits in spatial learning (Vukovic et al., 2013). Importantly, comparing aged sedentary and young ablated mice *in vivo* using our longitudinal multimodal MRI approach revealed the same overlapping, distinct changes in structural volume and circuitry, both of which are correlates that can be investigated in live human subjects.

Positive modulators of neurogenesis such as exercise have routinely been demonstrated to increase neurogenesis levels and improve spatial learning in aged rodents (van Praag et al., 2005), but due to the invasive and terminal nature of such experiments these have yet to be directly examined in human subjects. Instead, there is a reliance on correlates such as MRI perfusion and blood flow studies (Pereira et al., 2007). The data presented here demonstrate that *in vivo* changes in mouse hippocampal structure and function following an optimal period of exercise correlate to improvements in cognitive function and increased neurogenesis. Specific ablation of immature neurons during exercise prevented all of these positive changes. These findings provide mechanistic insight into how exercise activates otherwise quiescent neurogenesis and alters hippocampal structure and function as well as how immature neurons play a central role in these changes. Considering that MRI studies in humans have demonstrated correlations between hippocampal volume and/or connectivity and cognitive ability (De Marco et al., 2019; Lisofsky et al., 2015; Szymkowicz et al., 2016; Vecchio et al., 2017), we believe that our study offers a rational explanation for what may be occurring in the human brain following exercise and provides components that can be examined, especially in a longitudinal manner, to serve as useful indicators to optimize exercise in older adults to enhance cognitive function.

Taken together, our results indicate a direct relationship between neurogenesis and microstructural changes based on three lines of evidence. First, neurogenesis and structural changes coincide in the dorsal hippocampus following physical exercise. Second, there is a significant correlation between neurogenesis and structural changes. Third, to validate the causative effect of neurogenesis, we provide evidence that the structural and functional changes observed following exercise are abolished when neurogenesis is ablated. In future studies, the relationship between the structural plasticity of non-neuronal components and MRI changes should also be examined to determine their contribution to the observed macroscopic changes.

Conclusions

Neurogenesis alters the structure and functional circuitry in the hippocampus following exercise and ultimately results in cognitive improvement in aged animals (Figure 5). Specifically, neurogenesis decreases during aging, and results in hippocampal volume, MD, and connectivity deficits, as well as impaired learning. However, exercise can restore neurogenesis in old animals, which in turn restores the hippocampal volume and MD, resulting in significant changes in the strength of the connections in parts of the DG network, and improved learning. Our data bridge the gap between the microscopic and macroscopic

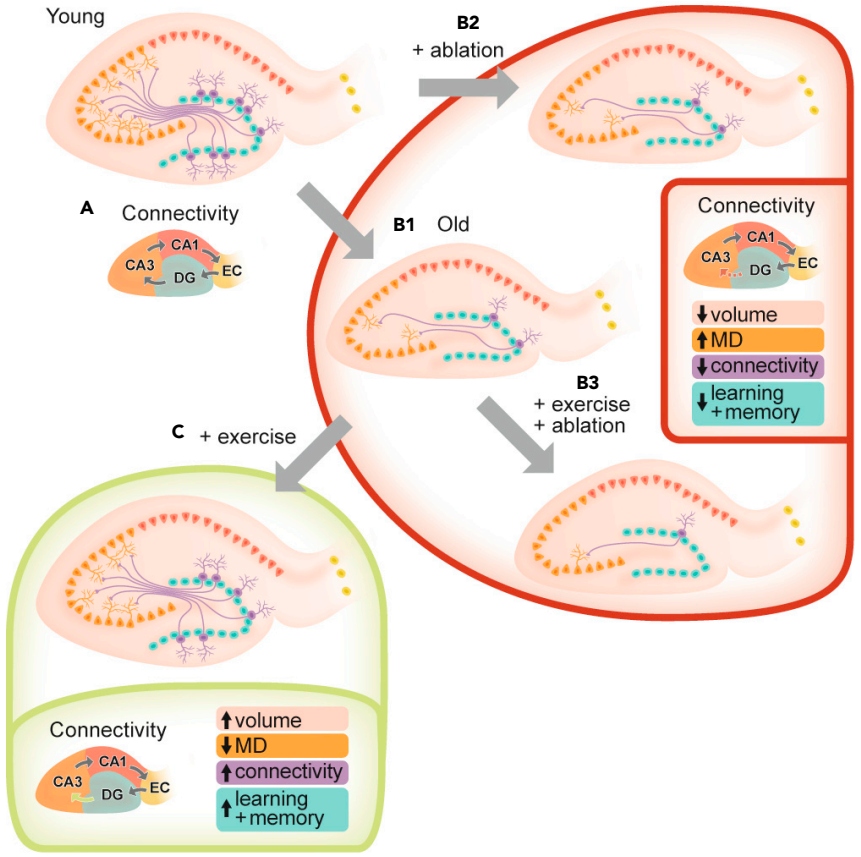

Figure 5. Schematic summarizing the changes in the dorsal hippocampus in response to aging, exercise, and neurogenesis ablation

(A) Information processing in the hippocampus occurs through a mostly unidirectional circuit, whereby projections from the entorhinal cortex (EC) via the perforant path connect to the DG, which in turn gives rise to mossy fibers that terminate within the CA3 region. Fibers projecting from CA3, termed Schaffer collaterals, innervate the CA1 region, which outputs to the subiculum and the EC.

(B) Neurogenesis in the DG decreases during aging **(B1)** and following ablation **(B2, B3)**, resulting in decreased hippocampal volume; increased MD, specifically interrupting the DG-CA3 connectivity; and eventually learning impairments.

(C) Exercise restores neurogenesis in old animals, which in turn restores the hippocampal volume, MD, and DG-CA3 connectivity and leads to improved learning ability.

levels of the hippocampus, linking hippocampal structure and connectivity with neurogenesis, and confirming that AHN is an essential driver of macroscopic changes in this region.

Limitations of the study

Only female mice were used in this study. When examining the effect of exercise in old animals, only healthy, 24-month-old female C57BL/6 mice without overt health issues were used. This was done to minimize separation of mice, which is more common for males as they fight. Young male and female mice have been reported to run different daily distances (Clark et al., 2011), and so the exact timing of physical exercise may be different between the sexes; however, previous studies indicate that this may not be the case. To determine if our findings can be generalized to both sexes or if there is a sex-dependent response to exercise in aged mice these experiments would need to be repeated in both sexes.

STAR★METHODS

Detailed methods are provided in the online version of this paper and include the following:

- KEY RESOURCES TABLE

SUPPLEMENTAL INFORMATION

Supplemental information can be found online at https://doi.org/10.1016/j.isci.2021.103450.

ACKNOWLEDGMENTS

This study was supported by National Health and Medical Research Council Project Grant (GNT1130141 to P.F.B. and D.G.B) and grant from the Stafford Fox Medical Research Foundation (P.F.B). We thank the staff of the University of Queensland Biological Resources Facility for breeding and maintaining the animals in this study, Rowan Tweedale and Megan Alexander for editorial assistance, and Nick Valmas for assistance with illustrations. Imaging was performed at the Queensland Brain Institute's Advanced Microscopy Facility. Behavioral tests were performed at the Queensland Brain Institute's Behavior and Surgical Facility. The authors acknowledge the 9.4-T MRI facility and scientific and technical assistance of the National Imaging Facility, a National Collaborative Research Infrastructure Strategy (NCRIS) capability, at the Center for Advanced Imaging, The University of Queensland.

AUTHOR CONTRIBUTIONS

X.A.Z., D.G.B., J.Z., X.T., N.D.K., A.C., and K-Y.V. performed the experiments, X.A.Z., D.G.B. and P.F.B. conceived the experiments, X.A.Z, D.G.B., F.N., K-H.C., T.J., and P.F.B analyzed the data and wrote the manuscript.

DECLARATION OF INTERESTS

The authors declare no competing interests.

Received: July 21, 2021
Revised: September 22, 2021
Accepted: November 10, 2021
Published: December 17, 2021

REFERENCES

Asan, L., Falfan-Melgoza, C., Beretta, C.A., Sack, M., Zheng, L., Weber-Fahr, W., Kuner, T., and Knabbe, J. (2021). Cellular correlates of gray matter volume changes in magnetic resonance morphometry identified by two-photon microscopy. Scientific Reports *11*.

Bernier, B.E., Lacagnina, A.F., Ayoub, A., Shue, F., Zemelman, B.V., Krasne, F.B., and Drew, M.R. (2017). Dentate gyrus contributes to retrieval as well as encoding: evidence from context fear conditioning, recall, and extinction. J. Neurosci. *37*, 6359–6371.

Berron, D., Neumann, K., Maass, A., Schutze, H., Fliessbach, K., Kiven, V., Jessen, F., Sauvage, M., Kumaran, D., and Duzel, E. (2018). Age-related functional changes in domain-specific medial temporal lobe pathways. Neurobiol. Aging *65*, 86–97.

Biedermann, S., Fuss, J., Zheng, L., Sartorius, A., Falfan-Melgoza, C., Demirakca, T., Gass, P., Ende, G., and Weber-Fahr, W. (2012). In vivo voxel based morphometry: detection of increased hippocampal volume and decreased glutamate levels in exercising mice. Neuroimage *61*, 1206–1212.

Biedermann, S.V., Fuss, J., Steinle, J., Auer, M.K., Dormann, C., Falfan-Melgoza, C., Ende, G., Gass, P., and Weber-Fahr, W. (2016). The hippocampus and exercise: histological correlates of MR-detected volume changes. Brain Struct. Funct. *221*, 1353–1363.

Bizon, J.L., and Gallagher, M. (2003). Production of new cells in the rat dentate gyrus over the lifespan: relation to cognitive decline. Eur. J. Neurosci. *18*, 215–219.

Blackmore, D.G., Steyn, F.J., Carlisle, A., O'Keeffe, I., Vien, K.Y., Zhou, X., Leiter, O., Jhaveri, D., Vukovic, J., Waters, M.J., et al. (2021).

An exercise 'sweet spot' reverses cognitive deficits of ageing by growth hormone-induced neurogenesis. iScience *24*, 103275.

Boldrini, M., Fulmore, C.A., Tartt, A.N., Simeon, L.R., Pavlova, I., Poposka, V., Rosoklija, G.B., Stankov, A., Arango, V., Dwork, A.J., et al. (2018). Human hippocampal neurogenesis persists throughout aging. Cell Stem Cell *22*, 589–599 e585.

Brun, V.H., Otnass, M.K., Molden, S., Steffenach, H.A., Witter, M.P., Moser, M.B., and Moser, E.I. (2002). Place cells and place recognition maintained by direct entorhinal-hippocampal circuitry. Science *296*, 2243–2246.

Buzsaki, G., and Moser, E.I. (2013). Memory, navigation and theta rhythm in the hippocampal-entorhinal system. Nat. Neurosci. *16*, 130–138.

Cahill, L.S., Steadman, P.E., Jones, C.E., Laliberte, C.L., Dazai, J., Lerch, J.P., Stefanovic, B., and Sled, J.G. (2015). MRI-detectable changes in mouse brain structure induced by voluntary exercise. Neuroimage *113*, 175–183.

Chuang, K.H., Lee, H.L., Li, Z., Chang, W.T., Nasrallah, F.A., Yeow, L.Y., and Singh, K. (2019). Evaluation of nuisance removal for functional MRI of rodent brain. Neuroimage *188*, 694–709.

Chuang, K.H., and Nasrallah, F.A. (2017). Functional networks and network perturbations in rodents. Neuroimage *163*, 419–436.

Cimadevilla, J.M., Fenton, A.A., and Bures, J. (2000). Functional inactivation of dorsal hippocampus impairs active place avoidance in rats. Neurosci. Lett. *285*, 53–56.

Clark, P.J., Brzezinska, W.J., Thomas, M.W., Ryzhenko, N.A., Toshkov, S.A., and Rhodes, J.S. (2008). Intact neurogenesis is required for benefits of exercise on spatial memory but not motor performance or contextual fear conditioning in C57BL/6J mice. Neuroscience *155*, 1048–1058.

Clark, P.J., Kohman, R.A., Miller, D.S., Bhattacharya, T.K., Brzezinska, W.J., and Rhodes, J.S. (2011). Genetic influences on exercise-induced adult hippocampal neurogenesis across 12 divergent mouse strains. Genes Brain Behav. *10*, 345–353.

Cooper, C., Li, R., Lyketsos, C., and Livingston, G. (2013). Treatment for mild cognitive impairment: systematic review. Br. J. Psychiatry *203*, 255–264.

Coughlan, G., Laczo, J., Hort, J., Minihane, A.M., and Hornberger, M. (2018). Spatial navigation deficits - overlooked cognitive marker for preclinical Alzheimer disease? Nat. Rev. Neurol. *14*, 496–506.

Creer, D.J., Romberg, C., Saksida, L.M., van Praag, H., and Bussey, T.J. (2010). Running enhances spatial pattern separation in mice. Proc. Natl. Acad. Sci. U S A *107*, 2367–2372.

De Marco, M., Ourselin, S., and Venneri, A. (2019). Age and hippocampal volume predict distinct parts of default mode network activity. Sci. Rep. *9*, 16075.

Denny, C.A., Kheirbek, M.A., Alba, E.L., Tanaka, K.F., Brachman, R.A., Laughman, K.B., Tomm, N.K., Turi, G.F., Losonczy, A., and Hen, R. (2014). Hippocampal memory traces are differentially modulated by experience, time, and adult neurogenesis. Neuron *83*, 189–201.

Erickson, K.I., Voss, M.W., Prakash, R.S., Basak, C., Szabo, A., Chaddock, L., Kim, J.S., Heo, S., Alves, H., White, S.M., et al. (2011). Exercise training increases size of hippocampus and improves memory. Proc. Natl. Acad. Sci. U S A *108*, 3017–3022.

Eriksson, P.S., Perfilieva, E., Bjork-Eriksson, T., Alborn, A.M., Nordborg, C., Peterson, D.A., and Gage, F.H. (1998). Neurogenesis in the adult human hippocampus. Nat. Med. *4*, 1313–1317.

Fan, X., Wheatley, E.G., and Villeda, S.A. (2017). Mechanisms of hippocampal aging and the potential for rejuvenation. Annu. Rev. Neurosci. *40*, 251–272.

Fanselow, M.S., and Dong, H.W. (2010). Are the dorsal and ventral hippocampus functionally distinct structures? Neuron *65*, 7–19.

Gomez, J., Barnett, M.A., Natu, V., Mezer, A., Palomero-Gallagher, N., Weiner, K.S., Amunts, K., Zilles, K., and Grill-Spector, K. (2017). Microstructural proliferation in human cortex is coupled with the development of face processing. Science *355*, 68–71.

Greicius, M.D., Krasnow, B., Boyett-Anderson, J.M., Eliez, S., Schatzberg, A.F., Reiss, A.L., and Menon, V. (2003). Regional analysis of hippocampal activation during memory encoding and retrieval: fMRI study. Hippocampus *13*, 164–174.

Jabes, A., Lavenex, P.B., Amaral, D.G., and Lavenex, P. (2010). Quantitative analysis of postnatal neurogenesis and neuron number in the macaque monkey dentate gyrus. Eur. J. Neurosci. *31*, 273–285.

Jung, M.W., Wiener, S.I., and McNaughton, B.L. (1994). Comparison of spatial firing characteristics of units in dorsal and ventral hippocampus of the rat. J. Neurosci. *14*, 7347–7356.

Keifer, O.P., Jr., Hurt, R.C., Gutman, D.A., Keilholz, S.D., Gourley, S.L., and Ressler, K.J. (2015). Voxel-based morphometry predicts shifts in dendritic spine density and morphology with auditory fear conditioning. Nat. Commun. *6*, 7582.

Kheirbek, M.A., Drew, L.J., Burghardt, N.S., Costantini, D.O., Tannenholz, L., Ahmari, S.E., Zeng, H., Fenton, A.A., and Hen, R. (2013). Differential control of learning and anxiety along the dorsoventral axis of the dentate gyrus. Neuron *77*, 955–968.

Koteja, P., Garland, T., Jr., Sax, J.K., Swallow, J.G., and Carter, P.A. (1999). Behaviour of house mice artificially selected for high levels of voluntary wheel running. Anim. Behav. *58*, 1307–1318.

Kronenberg, G., Bick-Sander, A., Bunk, E., Wolf, C., Ehninger, D., and Kempermann, G. (2006). Physical exercise prevents age-related decline in precursor cell activity in the mouse dentate gyrus. Neurobiol. Aging *27*, 1505–1513.

Le Bihan, D. (2014). Diffusion MRI: what the water molecule tells us about the brain. FEBS J. *281*, 2.

Leardini-Tristao, M., Andrade, G., Garcia, C., Reis, P.A., Lourenco, M., Moreira, E.T.S., Lima, F.R.S., Castro-Faria-Neto, H.C., Tibirica, E., and Estato, V. (2020). Physical exercise promotes astrocyte coverage of microvessels in a model of chronic cerebral hypoperfusion. J. Neuroinflammation *17*, 117.

Lesburgueres, E., Sparks, F.T., O'Reilly, K.C., and Fenton, A.A. (2016). Active place avoidance is no more stressful than unreinforced exploration of a familiar environment. Hippocampus *26*, 1481–1485.

Lester, A.W., Moffat, S.D., Wiener, J.M., Barnes, C.A., and Wolbers, T. (2017). The aging navigational system. Neuron *95*, 1019–1035.

Lisofsky, N., Martensson, J., Eckert, A., Lindenberger, U., Gallinat, J., and Kuhn, S. (2015). Hippocampal volume and functional connectivity changes during the female menstrual cycle. Neuroimage *118*, 154–162.

Livingston, G., Sommerlad, A., Orgeta, V., Costafreda, S.G., Huntley, J., Ames, D., Ballard, C., Banerjee, S., Burns, A., Cohen-Mansfield, J., et al. (2017). Dementia prevention, intervention, and care. Lancet *390*, 2673–2734.

Ma, X., Hamadeh, M.J., Christie, B.R., Foster, J.A., and Tarnopolsky, M.A. (2012). Impact of treadmill running and sex on hippocampal neurogenesis in the mouse model of amyotrophic lateral sclerosis. PLoS One *7*, e36048.

Marlatt, M.W., Potter, M.C., Lucassen, P.J., and van Praag, H. (2012). Running throughout middle-age improves memory function, hippocampal neurogenesis, and BDNF levels in female C57BL/6J mice. Dev. Neurobiol. *72*, 943–952.

Marstaller, L., Williams, M., Rich, A., Savage, G., and Burianova, H. (2015). Aging and large-scale functional networks: white matter integrity, gray matter volume, and functional connectivity in the resting state. Neuroscience *290*, 369–378.

Moon, H.Y., Becke, A., Berron, D., Becker, B., Sah, N., Benoni, G., Janke, E., Lubejko, S.T., Greig, N.H., Mattison, J.A., et al. (2016). Running-induced systemic cathepsin B secretion is associated with memory function. Cell Metab. *24*, 332–340.

Moser, E., Moser, M.B., and Andersen, P. (1993). Spatial learning impairment parallels the magnitude of dorsal hippocampal lesions, but is hardly present following ventral lesions. J. Neurosci. *13*, 3916–3925.

Moser, M.B., Moser, E.I., Forrest, E., Andersen, P., and Morris, R.G. (1995). Spatial learning with a minislab in the dorsal hippocampus. Proc. Natl. Acad. Sci. U S A *92*, 9697–9701.

Nakazawa, K., Quirk, M.C., Chitwood, R.A., Watanabe, M., Yeckel, M.F., Sun, L.D., Kato, A., Carr, C.A., Johnston, D., Wilson, M.A., et al. (2002). Requirement for hippocampal CA3 NMDA receptors in associative memory recall. Science *297*, 211–218.

Ngwenya, L.B., Heyworth, N.C., Shwe, Y., Moore, T.L., and Rosene, D.L. (2015). Age-related changes in dentate gyrus cell numbers, neurogenesis, and associations with cognitive impairments in the rhesus monkey. Front. Syst. Neurosci. *9*, 102.

Nyberg, L., and Pudas, S. (2019). Successful memory aging. Annu. Rev. Psychol. *70*, 219–243.

O'Leary, O.F., and Cryan, J.F. (2014). A ventral view on antidepressant action: roles for adult hippocampal neurogenesis along the dorsoventral axis. Trends Pharmacol. Sci. *35*, 675–687.

Pekcec, A., Baumgartner, W., Bankstahl, J.P., Stein, V.M., and Potschka, H. (2008). Effect of aging on neurogenesis in the canine brain. Aging Cell *7*, 368–374.

Pereira, A.C., Huddleston, D.E., Brickman, A.M., Sosunov, A.A., Hen, R., McKhann, G.M., Sloan, R., Gage, F.H., Brown, T.R., and Small, S.A. (2007). An in vivo correlate of exercise-induced neurogenesis in the adult dentate gyrus. Proc. Natl. Acad. Sci. U S A *104*, 5638–5643.

Reagh, Z.M., Noche, J.A., Tustison, N.J., Delisle, D., Murray, E.A., and Yassa, M.A. (2018). Functional imbalance of anterolateral entorhinal cortex and hippocampal dentate/CA3 underlies age-related object pattern separation deficits. Neuron *97*, 1187–1198 e1184.

Richards, K., Watson, C., Buckley, R.F., Kurniawan, N.D., Yang, Z.Y., Keller, M.D., Beare, R., Bartlett, P.F., Egan, G.F., Galloway, G.J., et al. (2011). Segmentation of the mouse hippocampal formation in magnetic resonance images. Neuroimage *58*, 732–740.

Sagi, Y., Tavor, I., Hofstetter, S., Tzur-Moryosef, S., Blumenfeld-Katzir, T., and Assaf, Y. (2012). Learning in the fast lane: new insights into neuroplasticity. Neuron *73*, 1195–1203.

Sahay, A., Scobie, K.N., Hill, A.S., O'Carroll, C.M., Kheirbek, M.A., Burghardt, N.S., Fenton, A.A., Dranovsky, A., and Hen, R. (2011). Increasing adult hippocampal neurogenesis is sufficient to improve pattern separation. Nature *472*, 466–470.

Salminen, L.E., Conturo, T.E., Laidlaw, D.H., Cabeen, R.P., Akbudak, E., Lane, E.M., Heaps, J.M., Bolzenius, J.D., Baker, L.M., Cooley, S., et al. (2016). Regional age differences in gray matter diffusivity among healthy older adults. Brain Imaging Behav. *10*, 203–211.

Sleiman, S.F., Henry, J., Al-Haddad, R., El Hayek, L., Abou Haidar, E., Stringer, T., Ulja, D., Karuppagounder, S.S., Holson, E.B., Ratan, R.R., et al. (2016). Exercise promotes the expression of brain derived neurotrophic factor (BDNF) through the action of the ketone body ß-hydroxybutyrate. Elife *5*, e15092.

Small, S.A., Schobel, S.A., Buxton, R.B., Witter, M.P., and Barnes, C.A. (2011). A pathophysiological framework of hippocampal dysfunction in ageing and disease. Nat. Rev. Neurosci. *12*, 585–601.

Sofi, F., Valecchi, D., Bacci, D., Abbate, R., Gensini, G.F., Casini, A., and Macchi, C. (2011). Physical activity and risk of cognitive decline: a meta-analysis of prospective studies. J. Intern. Med. *269*, 107–117.

Sorrells, S.F., Paredes, M.F., Cebrian-Silla, A., Sandoval, K., Qi, D., Kelley, K.W., James, D., Mayer, S., Chang, J., Auguste, K.I., et al. (2018). Human hippocampal neurogenesis drops sharply in children to undetectable levels in adults. Nature *555*, 377–381.

Spalding, K.L., Bergmann, O., Alkass, K., Bernard, S., Salehpour, M., Huttner, H.B., Bostrom, E., Westerlund, I., Vial, C., Buchholz, B.A., et al. (2013). Dynamics of hippocampal neurogenesis in adult humans. Cell *153*, 1219–1227.

Spalding, K.L., Bhardwaj, R.D., Buchholz, B.A., Druid, H., and Frisen, J. (2005). Retrospective birth dating of cells in humans. Cell *122*, 133–143.

Squire, L.R. (1992). Memory and the hippocampus: a synthesis from findings with rats, monkeys, and humans. Psychol. Rev. *99*, 195–231.

Strange, B.A., Witter, M.P., Lein, E.S., and Moser, E.I. (2014). Functional organization of the hippocampal longitudinal axis. Nat. Rev. Neurosci. *15*, 655–669.

Szymkowicz, S.M., Persson, J., Lin, T., Fischer, H., and Ebner, N.C. (2016). Hippocampal brain volume is associated with faster facial emotion identification in older adults: preliminary results. Front. Aging Neurosci. *8*, 203.

van Praag, H. (2008). Neurogenesis and exercise: past and future directions. Neuromolecular Med. *10*, 128–140.

van Praag, H., Christie, B.R., Sejnowski, T.J., and Gage, F.H. (1999a). Running enhances neurogenesis, learning, and long-term potentiation in mice. Proc. Natl. Acad. Sci. U S A *96*, 13427–13431.

van Praag, H., Kempermann, G., and Gage, F.H. (1999b). Running increases cell proliferation and neurogenesis in the adult mouse dentate gyrus. Nat. Neurosci. *2*, 266–270.

van Praag, H., Shubert, T., Zhao, C., and Gage, F.H. (2005). Exercise enhances learning and hippocampal neurogenesis in aged mice. J. Neurosci. *25*, 8680–8685.

Vecchio, F., Miraglia, F., Piludu, F., Granata, G., Romanello, R., Caulo, M., Onofrj, V., Bramanti, P., Colosimo, C., and Rossini, P.M. (2017). Small World" architecture in brain connectivity and hippocampal volume in Alzheimer's disease: a study via graph theory from EEG data. Brain Imaging Behav. *11*, 473–485.

Vivar, C., Peterson, B.D., and van Praag, H. (2016). Running rewires the neuronal network of adult-born dentate granule cells. Neuroimage *131*, 29–41.

Vukovic, J., Borlikova, G.G., Ruitenberg, M.J., Robinson, G.J., Sullivan, R.K., Walker, T.L., and Bartlett, P.F. (2013). Immature doublecortin-positive hippocampal neurons are important for learning but not for remembering. J. Neurosci. *33*, 6603–6613.

Wu, M.V., Luna, V.M., and Hen, R. (2015). Running rescues a fear-based contextual discrimination deficit in aged mice. Front. Syst. Neurosci. *9*, 114.

Yassa, M.A., Mattfeld, A.T., Stark, S.M., and Stark, C.E. (2011). Age-related memory deficits linked to circuit-specific disruptions in the hippocampus. Proc. Natl. Acad. Sci. U S A *108*, 8873–8878.

Yassa, M.A., Stark, S.M., Bakker, A., Albert, M.S., Gallagher, M., and Stark, C.E. (2010). High-resolution structural and functional MRI of hippocampal CA3 and dentate gyrus in patients with amnestic Mild Cognitive Impairment. Neuroimage *51*, 1242–1252.

STAR★METHODS

KEY RESOURCES TABLE

REAGENT or RESOURCE	SOURCE	IDENTIFIER
Antibodies		
4′,6-diamidino-2-phenylindole (DAPI)	Sigma-Aldrich	D9542
Guinea pig anti-DCX	Merck Millipore	RRID:AB_1586992
Goat anti-guinea pig Alexa Fluor-488	Molecular Probes	RRID:AB_2534117
Chemicals, peptides, and recombinant proteins		
Ketamine	Provet	Keti1
Xylazine	Provet	Xylaz2
Medetomidine	Dormitor®, Pfizer	149-109
Antiseden	Zoetis	40612/59805
Fluorescence anti-fade mounting medium	DAKO	S302380
Isoflurane	Henry Schein	988-3244
Diphtheria toxin	Sigma-Aldrich	D0564
NGS	Sigma	G9023
BSA	Sigma	A8412
Triton-X100	Sigma	T9284
Tween 20	Sigma	P1379
Experimental models: Organisms/strains		
C57BL/6J	The Jackson Laboratory	RRID:IMSR_JAX:000664
DCX^{DTR} knock-in mouse	Ozgene	Vukovic et al. (2013) J.Neurosci 33(15):6603-13
Software and algorithms		
Microsoft Excel	Microsoft	16.53
Prism	Graphpad	9.0
Australian Mouse Brain Mapping Consortium (AMBMC) brain template	Richards et al., 2011	(http://www.imaging.org.au/AMBMC/AMBMC)
SPSS	Microsoft	26
Other		
9.4 T horizontal bore animal scanner	Bruker BioSpin GmbH	N/A
PAP pen	Abcam	Ab2601
APA apparatus	Biosignal	N/A
MR-compatible rectal temperature probe	SA Instruments	SAII
infrared pulse oximeter sensor	SA Instruments	SAII

RESOURCE AVAILABILITY

Lead contact

Further information and requests for resources and reagents should be directed to and will be fulfilled by the lead contact, Perry Bartlett (p.bartlett@uq.edu.au).

Materials availability

This study did not generate unique reagents.

Data and code availability

- All data reported in this paper will be shared by the lead contact upon request.
- This paper does not report original code.
- Any additional information required to reanalyse the data reported in this paper is available from the lead contact upon request.

EXPERIMENTAL MODEL AND SUBJECT DETAILS

Animals

Adult female C57BL/6J mice up to 24 months of age were used throughout the study, unless otherwise stated. All animals were tested in accordance with the *Australian Code of Practice for the Care and Use of Animals for Scientific Purposes*. The University of Queensland Animal Ethics Committee approved all experiments. Animals were housed three or four per home cage. All animals had *ad libitum* access to food and water and were housed on a 12h light/dark cycle.

METHOD DETAILS

Exercise paradigm

Animals were housed three to a cage in boxes that were 50 cm long × 20 cm wide × 12.5 cm deep, with test animals given *ad libitum* access to a single hanging running wheel (Able Scientific) for defined periods of time. These exercise (''run'') periods were 21, 35, or 49 days. Control (''no run'') animals were housed in the same-sized boxes without a running wheel. A locked running wheel was not placed in these cage as this may have induced climbing and/or investigation, and hence may have qualified as environmental enrichment (Clark et al., 2008; Koteja et al., 1999).

Timeline of experimental procedures

The animals were tested two weeks after removal of the running wheel. Behavioral testing was conducted during the light phase. MRI scanning was conducted the day after cognitive testing had concluded. Animals were sacrificed immediately following the final MRI scan with brains prepared for immunohistochemical analysis.

Specific ablation of DCX^{+ve} cells

Female DCX^{DTR} knock-in mice at either 15 weeks or 24 months of age were used as previously described (Vukovic et al., 2013), to investigate the effect of specific ablation of newborn neurons following voluntary exercise. Briefly, animals underwent an initial round of active place avoidance (APA) testing to obtain their baseline spatial learning ability. They were then housed three to a cage and given *ad libitum* access to a running wheel for 35 days. After 28 days of exercise, diphtheria toxin (DT; Sigma) injections were initiated; 10 ng DT/g body weight was injected intraperitoneally every third day for a total of 6 injections. Body weight was measured daily. After 35 days of exercise, the running wheels were removed for 2 weeks prior to retesting of spatial learning ability using APA with novel cues.

MRI acquisition

All MR data were acquired in a 9.4 T horizontal bore animal scanner (Bruker BioSpin GmbH) equipped with a two element anatomically shaped cryogenic mouse head coil for transmission and reception. The mice were initially anesthetized with 2–3% isoflurane in air and O_2 (47% O_2) mixture. After securing the head in an MRI-compatible stereotaxic holder, 0.05 mg/kg medetomidine (Dormitor, Pfizer) was given intraperitoneally, after which sedation was maintained with 0.1 mg/kg/h continuous infusion and isoflurane was maintained at 0.4–0.8%. A low level of isoflurane (<0.5%), together with a low dose of medetomidine infusion, is considered to be the most robust anesthesia for detecting functional connectivity (Chuang and Nasrallah, 2017). Body temperature was maintained at 37.0 ± 0.5°C with an in-built warm water circulator and the cryoprobe surface heater, and monitored by an MR-compatible rectal temperature probe (SA Instruments). The breathing rate was monitored with a sensor pad (SA Instruments), with an average breathing rate of 110 ± 10.0 breaths/min. To ensure proper physiology under anesthesia, SpO_2 and heartbeat were measured using an MR-compatible infrared pulse oximeter sensor (SA Instruments) placed on the shaved left upper hindlimb in five of the animals, with an average SpO_2 of 96.5 ± 1.5% and an average heartbeat rate of 250.0 ± 50.0 beats per minute. For accurate and reproducible positioning, the head of the mouse

was fixed with a bite bar and a pair of ear bars in a stereotactic holder. Eye cream was applied to protect the animal's eyes and prevent them from becoming dry. The total time under anesthesia was less than 2.5 h for each animal.

Structural imaging. To measure brain structure and volume changes, high-resolution structural MRI scans were acquired using a T2-weighted RARE-sequence (Rapid Acquisition with Refocused Echoes) with the following parameters: TR/TE = 9000/20 ms, effective TE = 40 ms, resolution = 0.05 × 0.05 × 0.23 mm^3, matrix = 320 × 200 × 78 centered on the hippocampus, RARE factor = 4, and 2 averages. The total acquisition time was 6 min 32 s.

Diffusion tensor imaging (DTI). DTI was used to estimate microscopic tissue and white matter integrity changes. Scans were acquired with a diffusion-weighted spin-echo echo-planar-imaging (EPI) pulse sequence with the following parameters: TR/TE = 10,000/20.7 ms, δ/Δ = 4/10 ms, resolution = 0.2 × 0.2 × 0.2 mm^3, matrix = 80 × 50 × 78, 30 non-collinear gradient directions with a single b-value at 2000 s/mm^2 and two b-value of 0 s/mm^2 (referred to as b0). The total acquisition time was 10 min 40 s.

Functional connectivity imaging. Resting-state blood oxygenation level-dependent (BOLD) fMRI was used to measure the functional connectivity. It was consistently acquired 1.5h after the start of anesthesia when the physiology was most stable. BOLD fMRI data were acquired using a 2D gradient-echo EPI with the following parameters: TR/TE = 1000/10 ms, resolution = 0.23 × 0.26 × 0.5 mm^3, and matrix = 90 × 60 × 30. 600 volumes were acquired with a total acquisition time of 10 min.

MRI processing

All MRI data were pre-processed using FSL software (http://fsl.fmrib.ox.ac.uk/fsl).

Structural imaging. Tensor-based morphometric analysis was conducted on the structural MRI to estimate the volume changes in each voxel. T2-weighted images were first skull stripped by FSL-BET function, after which refined and manually modified. Field correction was performed by FSL-FAST to correct for field inhomogeneity. Linear and non-linear transformations were then applied with the FSL-FLIRT and FSL-FNIRT functions, respectively, to register the T2-weighted data to the resampled Australian Mouse Brain Mapping Consortium (AMBMC) brain template (http://www.imaging.org.au/AMBMC/AMBMC) (Richards et al., 2011). The study-specific template was made out of the registered images generated from all animals in each study. A second round of linear and non-linear transformation was then applied to register the T2-weighted data to the study-specific template. The Jacobian determinant map derived from this process was used as the estimate of volume change. The hippocampus was manually delineated on the AMBMC brain template and applied to the Jacobian determinant map to calculate the hippocampal volume.

Diffusion tensor imaging. Diffusion-weighted images were first motion and eddy current corrected with FSL-eddy function to realign different volumes to the b0 volume as a reference. Skull stripping was performed using the FSL-BET function and then refined and modified manually. Local fitting of diffusion tensors was performed with FSL-dtifit to obtain a matrix describing the orientation dependence in each voxel and the eigenvalues and eigenvectors of the diffusion tensor, which were further used to calculate the mean diffusivity (MD). Linear and non-linear registration were then applied to register b0 images to the AMBMC MRI template using FSL-FLIRT and FSL-FNIRT, after which a study-specific DTI template was constructed from the registered images. A second round of linear and non-linear registration was conducted to register the DTI data to the study-specific DTI template. The transformation was then applied to the MD maps.

Functional connectivity imaging. Resting-state fMRI images were first skull stripped by FSL-BET and then refined manually. Nuisance regression was performed by regressing 10 principal components of the time series outside the brain, motion repressors (estimated by FSL-mcflirt) and the quadratic trend that models the baseline signal drift (Chuang et al., 2019). For registration, the averaged EPI of each animal was first field inhomogeneity corrected by FSL-FAST and then registered to its own structural MRI scan, followed by linear and non-linear transformation by ANTs (http://stnava.github.io/ANTs/) to the AMBMC brain template. An fMRI study-specific template was then constructed from the registered images. A second round of linear and non-linear transformation was applied to register the fMRI data to the study-specific template. After registration, the data were bandpass filtered at 0.01–0.3 Hz, followed by minimal

spatial Gaussian smoothing (FWHM = 0.23 mm) to avoid reducing the high spatial resolution. Seed-based correlation analysis was applied to estimate the functional connectivity between pre-defined regions of interest (ROIs) that partitioned the hippocampus into 10 sub-regions (Figure S5), including the medial and lateral entorhinal cortex, dorsal and ventral DG, dorsal and ventral CA1, dorsal and ventral CA3, and dorsal and ventral subiculum. The correlation was then converted to a *Z* score by Fisher's z-transformation for further group-wise statistical tests.

Spatial learning

Animals were handled daily for 4 days prior to the initiation of behavioral tests. They were placed in a clear plastic cylinder (1 meter diameter) on a gridded platform (Biosignal) rotating at 1 revolution per min. A 5 min habituation session with no shocks was conducted on the first day, and 10 min testing sessions were conducted for the following 5 days. During the testing sessions, a 60° area was denoted by the tracking computer; animals were tracked automatically and if an animal entered this exclusion area it received a 0.5 mA shock with a 500 ms latency. The inter-shock latency was 1,500 ms. Visual cues were spaced evenly around the room, and the animal was placed into the arena at the same position on each day of testing. At the conclusion of testing, animals were randomly assigned to control (no run or vehicle injection) or treatment (running wheel or DT injection) groups. At the conclusion of the experimental paradigms, the animals were again tested on the APA platform. In the retest phase, the visual cues were replaced with novel cues but the shock zone remained in the same location. For retesting, novel visual cues were used, the habituation day was omitted and there were 5 testing days. Visual data collection for the animals was achieved via a ceiling-mounted video camera connected to the tracking and shock computer. Between testing of each animal, the grid and platform were thoroughly cleaned with 80% ethanol. Parameters including distance traveled, speed and number of shocks were all recorded automatically. To calculate learning ability during the APA task we calculated the number shocks between the first day of testing to the last and expressed this as a percentage. Prior to all experiments, any animal with cataracts was excluded.

Tissue processing and immunohistochemistry

Animals were deeply anesthetized with sodium pentobarbitone. They were then transcardially perfused with ice-cold phosphate-buffered saline (PBS) followed by 4% paraformaldehyde in PBS (pH 7.4). Brains were removed, post-fixed overnight at 4°C in 4% paraformaldehyde and then placed in 30% sucrose solution. Serial brain coronal sections were cut at a thickness of 50 μm and placed in a six-series configuration. All sections were placed in PBS, washed and stored at 4°C in PBS +0.01% sodium azide until used.

Brain tissue sections were processed and labeled for the detection of DCX and DAPI. Sections were washed three times with PBS prior to incubation with blocking solution (PBS/0.2% Triton X-100/2% normal goat serum) for 60 min at room temperature (RT). They were then washed three times in PBS and incubated overnight at 4°C on a shaking platform with guinea pig anti-DCX (1:1,000; Merck), after which they were again washed three times prior to the addition of goat anti-guinea pig Alexa Fluor 488 (1:1,000; Invitrogen) for 2 h on a shaking platform at RT in the dark. The sections were then washed, with DAPI (1:10,000) being added after the second wash, before being mounted on Superfrost Plus slides. Once the excess liquid had dried, fluorescence anti-fade mounting medium (DAKO) was added and a coverslip applied. The sections were viewed using an x20 objective on an upright Zeiss Axio Imager Z1 fluorescence microscope. Mosaic images of the hippocampus were taken using the DAPI filter and the DG length was calculated using ZEN image analysis software (Zeiss). To estimate the volume of the DG, the boundaries of the granule cell layer (GCL)/subgranule cell layer (SGL) were outlined in every DAPI-labelled section in a 1 in 6 series throughout the dorsal hippocampus. The sum of the outlined GCL/SGL areas per animal was then multiplied by six and by section thickness (40μm) to estimate the total volume according to the Cavalieri principle (Salminen et al., 2016). The cell density was estimated by dividing the total cell counts by the volume.

QUANTIFICATION AND STATISTICAL ANALYSIS

Repeated measures (RM) two-way analysis of variance (ANOVA) with a false discovery rate (FDR) multiple comparison *post hoc* test or a Student's t-test was used to analyze data, as appropriate. Pearson correlation was applied to the correlation analysis. Parameters were analyzed in SPSS and Prism 9 (Graphpad Software Inc.). All values are expressed as mean ± standard error of the mean, unless otherwise indicated.